The Edge Operational Space in JET

J Lingertat, V Bhatnagar, G D Conway, L-G Eriksson,
K Günther, M von Hellermann, M Mantsinen[1], V Parail,
R Prentice, G Saibene, R Smith, K-D Zastrow.

JET Joint Undertaking, Abingdon, Oxfordshire, OX14 3EA,
[1] Also at: Helsinki University of Technology, Association Euratom-Tekes, Finland.

ABSTRACT

In this paper we investigate differences of the ELM behaviour between RF and NB heated H-mode discharges in JET. The main result of this investigation is that the edge pedestal pressure with NB heating is higher than with RF heating for equal power fluxes crossing the separatrix. This can be explained by a higher population of fast ions in the edge region in the case of NB heating. Using data from NB heated steady-state H-modes we derive a scaling law for the width of the transport barrier. We find that the barrier width is proportional to the poloidal Larmor radius, which in turn is controlled by the ion population with the highest energy in the plasma edge.

1. INTRODUCTION

The quality of tokamak H-mode discharges depends sensitively on parameters of the edge plasma. This led recently to a representation of tokamak discharges as an edge density - edge temperature plot, which is called the edge operational diagram [1 - 6]. The edge diagram shows boundaries which limit the achievable performance of the main plasma in terms of confinement, density and ELM behaviour and define the operational space for a specific device.

An important and rigid limit in the edge diagram is given by the maximum edge pressure gradient. It is well known that in an H-mode discharge a transport barrier with a width Δ exists inside the separatrix which causes a region of steep pressure gradient, the edge pedestal, to form. Assuming the pedestal width Δ to be constant, the edge pressure gradient limit appears in the edge diagram as a hyperbolic curve. Each time the discharge trajectory reaches this limit an ELM is triggered which reduces the pressure. Subsequently, the pressure recovers and after a time $\tau = 1/f_{ELM}$, where f_{ELM} is the ELM frequency, the limit is reached again. In this way an H-mode discharge evolves into a quasistationary state characterised by the magnitude of the edge pressure limit, by the amount of pressure drop during an ELM and by the frequency of ELM occurrence. The extrapolation of this limit and of the associated ELM parameters to future next step devices such as ITER is essential and requires an understanding of the physics involved.

Therefore a series of experiments was carried out in JET to characterise the pressure gradient limit and the ELM phenomenon. The experiments and their results will be discussed in this paper.

The paper begins with a comparison between neutral beam (NB) and radio-frequency (RF) heated H-modes, shows results obtained for the isotope scaling of the edge pedestal width and describes specific experiments performed to clarify the physical mechanisms which control the transport barrier.

2. THE EDGE PRESSURE GRADIENT LIMIT

The edge pressure gradient limit is generally assumed to be caused by the ballooning instability [7]. However, there is experimental and theoretical evidence that the outer kink mode is involved, if not controlling the limit and therefore the occurrence of the ELM. Plasma current (I_p) ramp-up and ramp-down experiments were used during steady-state H-modes to investigate the influence of an induced edge current on the ELM behaviour [8]. Ramping the current up, i.e. increasing the edge current density, drives the discharge to a state of small ELMs and into L-mode, ramping the current down triggers an immediate transition into an ELM-free phase. Even the smallest practically feasible ramp rates (dI_p/dt ~30 kA/s) have this effect. MHD stability calculations for typical JET discharges show that in most cases the kink limit is reached before the ballooning limit [9], but the ELM is triggered after the discharge trajectory moves further into the direction of the ballooning limit.

We assume in the following that the ballooning instability is responsible for the edge pressure gradient limit —p^{crit} and use the simple relation

$$\nabla p^{crit} \propto I_p^2 \cdot S^y \tag{1}$$

where S is the magnetic shear [10]. The exponent y has been introduced to allow for the fact that expression (1) with y = 1 is valid for circular magnetic surfaces and large aspect-ratio only. Equation (1) is simplified further by replacing ∇p^{crit} with p^{crit}/Δ:

$$p^{crit} \propto I_p^2 \cdot S^y \cdot \Delta \tag{2}$$

This simplification is necessary to allow a comparison with experimental data since the pressure gradient itself or the pedestal width Δ are experimentally not accessible at JET. Instead, either the electron pressure p_e or both the electron and ion pressure ($p_{tot} = p_e + p_i$) are measured at the top of the pedestal at R = 3.75 m ($\rho \sim 0.9$), using an interferometer for n_e, an electron cyclotron radiometer for T_e and charge-exchange spectroscopy for T_i and n_i measurements. The assumption $p_e = p_i$ is made if only p_e data are available. Sometimes for Δ the electron temperature pedestal width Δ_{Te} , obtained from ECE measurements, is used. However, there is no basis to assume an equality between Δ and Δ_{Te}. On the contrary, data analysis in JET shows a different behaviour of Δ_{Te} and Δ_{Ti} with increasing T_e and T_i [11], and values for Δ_{ne} and Δ_{ni} on which Δ also depends are not available for JET.

Equation (2) is used in this paper to investigate the scaling of Δ by assuming that different mechanisms are responsible for the formation of the transport barrier.

3. COMPARISON BETWEEN NB AND RF HEATED H-MODE DISCHARGES

Generally, RF heated H-modes in JET show, in comparison to NB heated ones, benign small high frequency ELMs [12]. In Fig. 1 two typical discharges are compared for which all parameters are held constant and only the heating method is different. The heating scenario for the RF

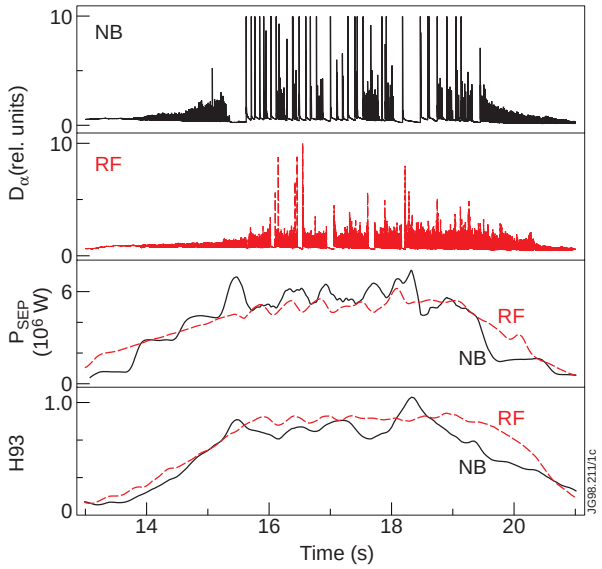

Fig. 1 Comparison between NB and RF heated H-modes, #42524, #42525.

case is ion cyclotron hydrogen minority heating with a resonance in the centre of the plasma. Both discharges have approximately the same power crossing the separatrix (P_{sep}) and a similar confinement characterised by the H93 factor [13]. P_{sep} is defined as the difference between the input power and that lost by radiation from the bulk plasma, and in the case of NB heating, the shine-through fraction and the fast ion charge-exchange losses are taken into account.

Figure 2 shows the same discharges in more detail together with the edge electron pressure p_e and the central electron temperature of the RF heated pulse. After the L-H

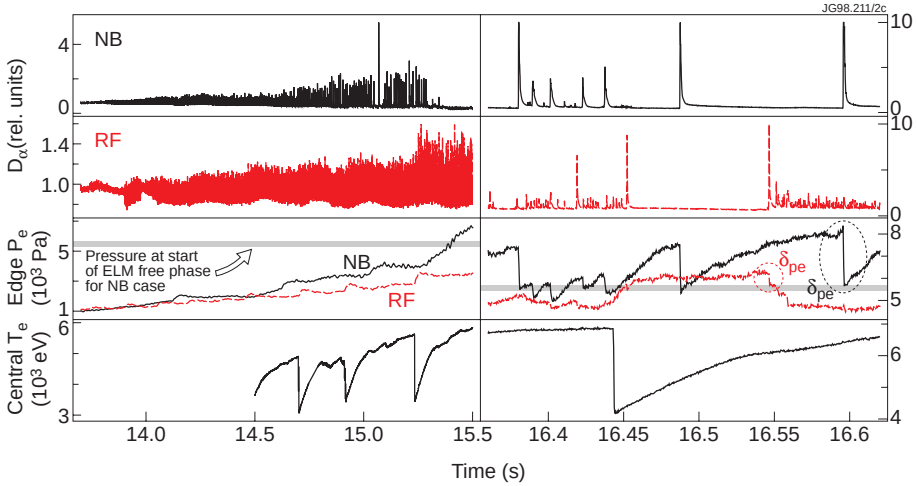

Fig. 2 Details of the same discharges as in Fig. 1.

transition both discharges evolve initially in the same way. The ELM frequency is high (transition ELMs) and decreases continuously. Simultaneously, the ELM size increases together with p_e and the total stored energy. From measurements on ASDEX it is known that during this phase the width of the density pedestal increases [7]. This increase continues until the first type I ELM appears after the ELM free period. Furthermore, the time evolution of the electric field in the pedestal region, obtained by analysing the fast neutral losses in ASDEX Upgrade, supports the assumption of an increasing width during this initial period of an H-mode discharge [14]. Additional support comes from modelling results obtained with the JETTO code [6]. These results show that a decreasing ELM frequency simultaneously with increasing ELM amplitude and stored energy can under the assumption of a pressure gradient limited MHD instability be obtained only by increasing the width of the transport barrier. In Fig. 1 the NB heated discharge

enters at ~15.4 s the ELM free phase, and at ~15.7 s the steady state type I ELM phase. From previous analysis of JET discharges we know that D varies weakly during the type I ELM phase [2].

The RF heated discharge deviates significantly from the NB heated one from ~14.5 s onwards: p_e stays throughout the discharge below the one for the NB case, despite the fact that the power which crosses the separatrix is the same for both cases. Assuming that the pressure gradient limit is the same, we have to conclude that the width of the transport barrier for the RF case remains smaller. One of the consequences is the higher frequency and smaller amplitude of ELMs in RF heated H-modes.

Figure1 shows for the RF heated discharge a few short ELM free phases accompanied by larger ELMs. In Fig. 2 one of these phases is shown in more detail. It is obvious that they are correlated with the occurrence of sawteeth. Sawteeth eject energy from the plasma centre and a heat wave travels to the plasma edge. It is seen in Fig. 2 as a transient increase of p_e between 16.45 s and 16.55 s. Interestingly, the value of p_e at which the ELM free phase starts is approximately the same for both heating methods. The occurrence of an ELM free phase together with an increase of the edge pressure can only be explained by a simultaneous and faster increase of Δ, so that the pressure gradient drops below its critical value ∇p^{crit}. There are two possible explanations for this increase in Δ. Assuming a dependence of Δ on the poloidal Larmor radius as shown in [2] the pedestal width may simply increase due to an increase in T_i during the sawtooth generated heat pulse. However, the dependence of Δ on T_i is weaker than the dependence of the edge pressure on T_i, so that the ratio should increase. Another explanation is based on the well established fact that during a sawtooth fast particles are ejected from the plasma centre and deposited in the outer plasma region [15]. Assuming that the relevant Larmor radius responsible for the width of the transport barrier is determined by the fastest component of the ion population, the observed occurrence of an ELM free phase after a sawtooth can easily be understood. The importance of the fast ion concentration is discussed later.

The value to which p_e increases after the sawtooth is still well below the value for the NB case as can be seen in Fig. 2. The critical p_e at which the NB heated discharge triggers ELMs is much higher, and the size of the ELM in terms of p_e drop per ELM (δp) remains a factor of 4-6 smaller than during NB heating.

Following the argument that the RF heated discharge has frequent and small ELMs due to a narrower pedestal width, we should expect the stored energy to be smaller compared to the NB case. However, as Fig. 1 shows, the confinement for both heating scenarios is approximately the same. The reason is the more peaked central pressure profile obtained with RF heating. Figure 3 shows the main plasma electron density, temperature and pressure profiles obtained from LIDAR [16] measurements for the same discharges as those used in Figs.1 and 2. The density profiles for both discharges are very similar with the exception of a slightly stronger peaking with NB heating due to central particle fuelling. The electron temperature and pressure profiles are however, more peaked for the RF case. Figure 4 shows the calculated power

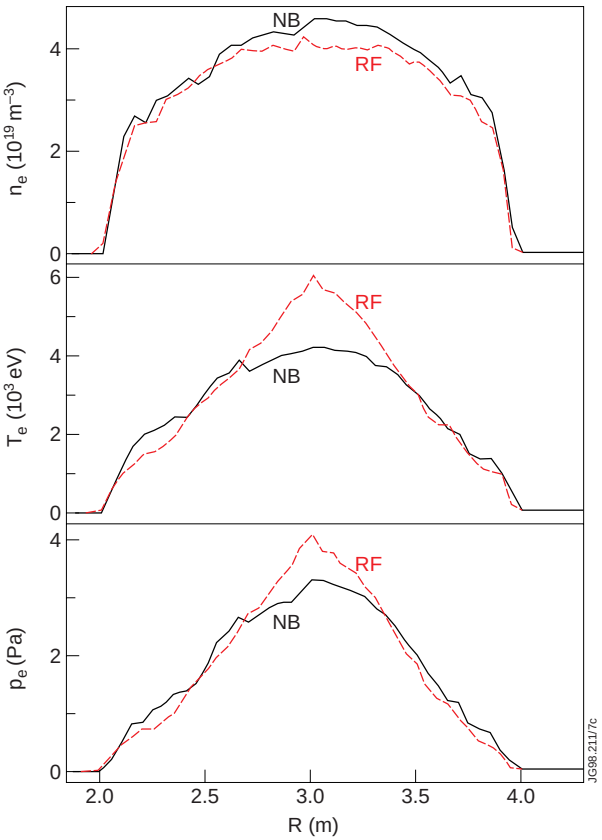

Fig. 3 Core plasma profiles of electron density, temperature and pressure for the same two discharges as in Fig.1. The profiles are averaged over the steady-state ELMy phase. The spatial resolution is ΔR~10 cm.

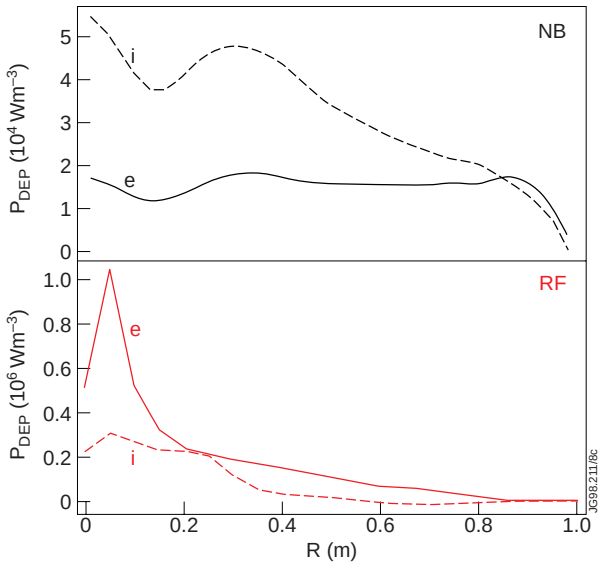

Fig. 4 Power deposition profiles for the same two discharges as in Fig. 1. The profiles were calculated using the CHEAP [17] and PION [18] code.

deposition profiles for both discharges. In the case of RF the heating, in particular of the electron component, is concentrated in the plasma centre. This observation leads to the conclusion that the confinement of the RF heated plasma is improved by a more central power deposition compared to the NB case.

To prove this hypothesis two discharges were modelled using the JETTO code [6], one NB heated with power deposition profiles taken from a discharge and one RF heated with an artificial power deposition profile, simulating the observed peaking of power deposition. One result of the modelling, the confinement time as a function of time, is shown in Fig. 5. For the RF case two different assumptions were made about the existence of a pressure

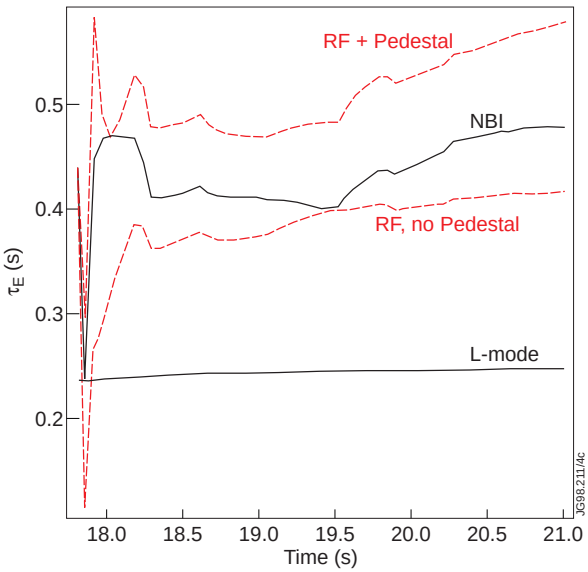

Fig. 5 Simulated energy confinement time as a function of time.

pedestal: the same pressure pedestal as the NB case and no pressure pedestal. The result shows that indeed the peaked power deposition profile improves the confinement and that in order to reproduce the NB confinement a small pressure pedestal is required for the RF case.

4. SCALING OF THE EDGE PEDESTAL WIDTH

In [2] the edge pedestal width scaling for NB heated discharges was investigated by varying n_e and T_e and by trying to fit the resulting trajectory in the n_e - T_e diagram assuming different physical mechanisms controlling Δ. The conclusion was that the experimental data are best fitted by $\Delta \propto \rho^x$ where ρ is the poloidal Larmor radius and x is between 1/2 and 2/3. All experiments were performed using deuterium. In the 1997 campaign tritium and hydrogen were also available, so that the scaling $\Delta \propto \rho^x$ could be further tested for NB heated discharges by investigating the dependence of Δ on the isotope mass A. We used Eq. (2) and tested Δ for six different expressions of the form

$$\Delta \propto \left(\frac{\sqrt{A \cdot T}}{I_p}\right)^x \qquad (3)$$

with x = 1, 1/2, 2/3 and $T = T_{i,\,thermal}$ or $T = \langle E \rangle_{fst}$ where $\langle E \rangle_{fst}$ is the average energy of fast particles at R = 3.75 m obtained from the CHEAP code [17]. $\langle E \rangle_{fst}$ was in the range of 11.5 keV to 88.4 keV. Additionally, all other parameters in Eqs. (2) and (3) were varied as much as practically possible: I_p between 1.8 and 3 MA, S between 2.98 and 3.95 and A between 1 and 3. S was taken from EFIT calculations. No gas puffing was used in these discharges. Here we show the main result in Fig. 6. The best fit is obtained assuming the fast particles determine ρ, a proportionality between Δ and ρ (x = 1) and a quadratic dependence of p_{tot} on S (y = 2). The standard deviation of the data from the regression line shown in Fig.6 is $\sigma \sim 3\%$. All other cases tested have a $\sigma \geq 10\%$ and the variation of σ with S shows a minimum around S = 2.

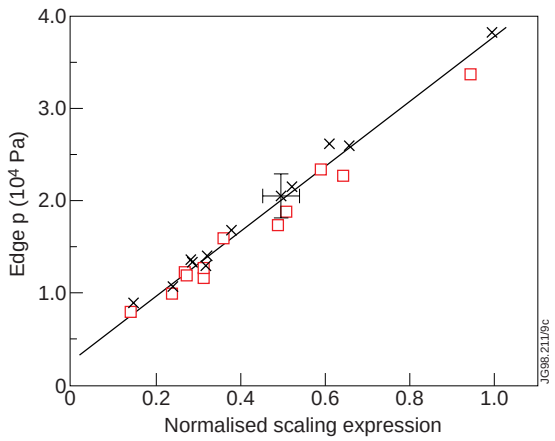

Fig. 6 Total pedestal plasma pressure (p_e+p_i) as a function of the normalised scaling parameter $I_p \cdot S^2 \cdot \sqrt{A \cdot \langle E \rangle_{fst}}$. × - data are maximum values, 1 - data are averaged values.

The above result has a major deficiency. Obviously, a single fast particle will not change the transport barrier. This means that in the investigated scaling law for Δ (Eq. 3) a parameter is missing which is controlled by the concentration of the fast particles. The reason for this deficiency is the lack of a suitable theoretical model which contains all relevant parameters. Work for developing such a model is under way. Here we restrict ourselves to the qualitative statement

that Δ is controlled by the ion population with the highest energy, provided their density is larger than some unknown threshold.

The assumption that fast ions control the pedestal width in the case of NB heating explains in a straightforward manner the difference between RF and NB H-modes in JET. With NB heating fast ions are produced right in the edge whereas with RF heating the source of fast ions is located at the resonance position in the plasma centre. For RF heated plasmas, calculation of the fast ion distribution at the edge results in very large error bars, due probably the inadequate consideration of fast ion transport and badly known input parameters for the PION code [18]. Therefore we performed specific experiments to investigate the role of fast particles in RF heated discharges, which are described in Section 5.

Another observation which supports the relevance of the fast particle population is the mass dependence of the critical edge pressure. Whereas the NB heated plasmas show a clear increase of p^{crit} with the mass of the beam ions, RF discharges show p^{crit} to be independent of A. In the RF experiments analysed hydrogen was always used as the heated minority, independent of the background gas which was varied from 100% D to 95% T: that means the mass of the fast particle component has not changed.

5. EDGE HEATING EXPERIMENTS WITH RF

Three types of edge RF heating experiments were performed (see Table I):

- the frequency of 3 of the 4 RF generators was changed in such a way to shift the location of the resonance for 75% of the power towards the high field edge (H minority),
- the phasing of the antennae was changed to widen the deposition profile of the fast particles (H minority),
- the magnetic field was slightly changed to create a He^3 resonance near the low field edge.

All three cases have reference discharges with central heating only as shown in Table I. The RF specific details of the phasing experiment are described elsewhere [19]. As an example the corresponding fast pressure profiles are shown in Fig. 7. The existence of fast particles at the edge during discharges with edge heating is experimentally established using data obtained with the neutral particle analyser. Figure 8 compares two energy spectra of the efflux of neutrals for the last pair of discharges in Table I. Clearly, the particle flux for energies larger than ~30 keV increases if edge heating is applied.

For each pair of discharges in Table I three ELM parameters are compared; ELM frequency, edge electron pressure and particle loss per ELM. The last parameter, obtained by a divertor interferometer, is used as a qualitative measure of the ELM strength since more conventional measures such as the stored energy or edge pressure drop are too small to be reliably measured.

Heating location	No.	Maj.	Min.	Phasing	R_{res}(m)	f_{ELM} (s^{-1})	p_e(edge) (10^3 Pa)	δN/ELM (10^{16})
Central	41514	D	H/1	+90°	2.81	2150-2200	4.3	1.3
Central: 25% Edge: 75%	41519	D	H/1	+90°	2.81 2.50	470-540	5.8	4.2
Central	41514	D	H/1	+90°	2.81	2150-2200	4.3	1.3
Central	41515	D	H/1	-90°	2.81	517-575	6.2	4.1
Central	42772	T	D/1	180°	3.02	1250-1650	5.6	0.6
Central: 30% D minority Edge: 70% He^3 minority	41754	T	D/1 He^3	180°	2.81 3.75	90-250	7.1	2.0

Table 1 ICRH experiments (Maj. - majority ions, Min. - heated minority ions)

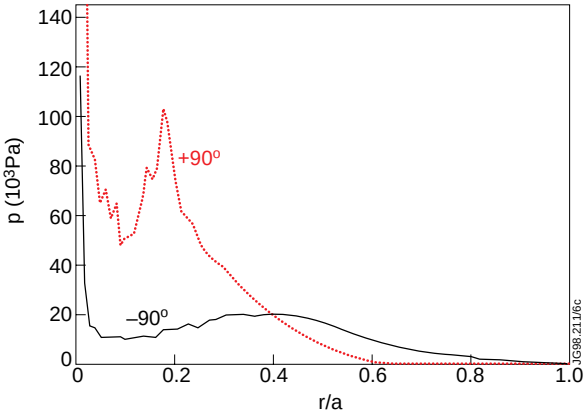

Fig.7 Calculated fast ion pressure profiles for two RF heated H-modes with +90° and -90° phasing (see Table 1), #41514, #41515.

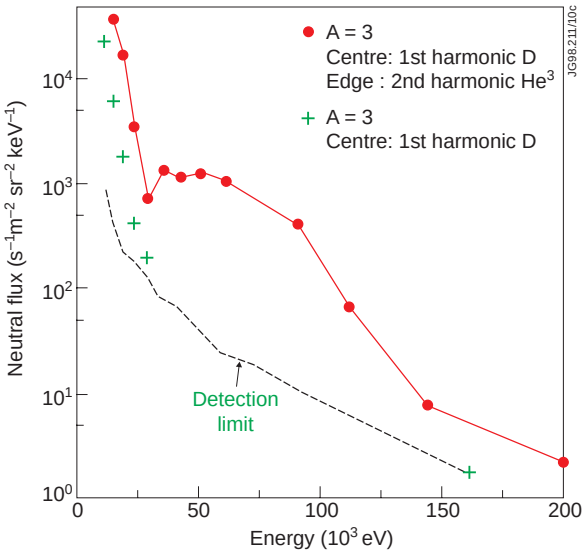

Fig.8 Energy spectra of neutral He^3 for two discharges, one with central heating only, the other with additional edge heating (see Table 1), #42772, #41754.

All three pairs of discharges show the same behaviour. Putting more fast particles into the edge reduces the ELM frequency, increases p_e at which ELMs are triggered and increases the strength of the ELM. However, none of the edge heated discharges show a type I ELMy phase with an ELM frequency around 10 s^{-1} as found in NB heated discharges in deuterium or tritium. This fact again supports the fast particle concept. In the first two pairs of RF heated discharges (Table I) fast hydrogen ions are created. Therefore they have to be compared to NB cases with hydrogen injection which due to the low mass of hydrogen stay mostly in the transition ELM regime. In the third pair He^3 ions are heated at the edge which have a Larmor radius near to that of H ions.

6. SUMMARY AND CONCLUSIONS

In this paper we assume that a unique MHD instability controls the maximum achievable edge pressure gradient ∇p^{crit} throughout the H-mode phase. Then the evolution of the ELM parameters in terms of frequency and strength and of the total stored energy of the plasma can be understood qualitatively as a variation of the width Δ of the transport barrier. Since, on JET, Δ is not directly measured, all statements and conclusions related to Δ are based on studies of its scaling with measurable parameters.

Starting with the L-H transition Δ increases during the transition ELM and the ELM free phase. With the onset of the steady-state ELMy phase (type I ELMs) Δ is nearly constant and depends only weakly on the pedestal plasma parameters. For this phase the experimentally determined scaling of the critical pedestal total pressure in the case of NB heated H-modes is

$$p^{crit} \propto I_p \cdot S^2 \cdot \sqrt{A \cdot < E >_{fst}} \ ,$$

where $<E>_{fst}$ is the average energy of fast ions in the pedestal region. The scaling implies a proportionality between Δ and the poloidal Larmor radius which in turn is controlled by the energy of the fastest ion population. This result needs further confirmation and dedicated experiments are planned for the next JET campaign. Its implications for future tokamak experiments are the possibility to control Δ by shallow NB injection, and an influence of the α-particle population on Δ in the case of an ignited plasma.

RF heated H-modes in JET (H minority heating in the plasma centre) exhibit a smaller edge pedestal pressure compared to similar NB heated ones, leading to smaller, more frequent ELMs. They stay in the transition ELM regime, because the concentration of fast particles at the edge is small. Despite a smaller edge pedestal the resulting total confinement of RF heated discharges equals NB heated equivalent discharges. This is consistent with the more peaked power deposition profile in the case of RF heating.

ACKNOWLEDGMENT

The authors gratefully acknowledge support from the Task Forces and from the Divertor Physics Topic Group.

REFERENCES

[1] M. Kaufmann et al., 16th IAEA Conference, Montreal (1996) F1-CN-64/O1-5.

[2] J. Lingertat et al., 24th EPS Conf. on Controlled Fusion and Plasma Physics, Berchtesgaden (1997) Or01, relevant material published in [3,6].

[3] M. Keilhacker et al., Plasma Physics and Controlled Fusion 39 (1997) B1.

[4] T.H. Osborne et al., 24th EPS Conf. on Controlled Fusion and Plasma Physics, Berchtesgaden (1997) Vol. 3, 1101.

[5] G. Janeschitz et al., 24th EPS Conf. on Controlled Fusion and Plasma Physics, Berchtesgaden (1997) Vol. 3, 993.
[6] A. Taroni et al., Contributions to Plasma Physics 38 (1998) 37.
[7] F. Wagner et al., 13th IAEA Conference, Washington (1990) Vol.1, 277.
[8] J. Lingertat, ELM characteristics and power deposition in JET, ASDEX Upgrade -JET Edge Physics Workshop, 3 - 4 Feb. 1997, JET Joint Undertaking.
[9] G.T.A. Huysmans et al., Nucl. Fusion 38 (1998) 179.
[10] D. Dobrott et al., Phys. Rev. Lett. 39 (1977) 943.
[11] P. Breger et al., Plasma Phys. Contr. Fusion 40 (1998) 347.
[12] V.P. Bhatnagar et al., 24th EPS Conf. on Controlled Fusion and Plasma Physics, Berchtesgaden (1997) Vol. 1, 77.
[13] K. Thomsen et al., Nucl. Fusion 34 (1994) 131.
[14] W. Herrmann, 22nd EPS Conf. on Controlled Fusion and Plasma Physics, Bournemouth (1995) Vol. 1, 333.
[15] G. Sadler et al., Fusion Technology 18 (1990) 556.
[16] C. W. Gowers et al., Rev. Sci. Instrum. 66 (1995) 475.
[17] M. G. von Hellermann et al. in Diagnostics for Experimental Thermonuclear Fusion Reactors, Plenum Press, New York and London (1996) p. 281 ff.
[18] L.-G. Eriksson et al., Nucl. Fusion 33 (1993) 1037.
[19] M. Mantsinen et al., 2nd Europhysics topical conference on RF Heating and current drive of fusion devices, Brussels, 20-23 January 1998.